TU/e EINDHOVEN UNIVERSITY OF TECHNOLOGY

CAD-tool for integrated optics

Citation for published version (APA):
Leijtens, X. J. M., Spiekman, L. H., Dam, van, C., Vreede, de, L. C. N., Smit, M. K., & Tauritz, J. L. (1995). CAD-tool for integrated optics. In L. Shi, L. H. Spiekman, & X. J. M. Leijtens (Eds.), *7th European Conference on Integrated Optics with Technical Exhibition : ECIO '95 : Regular and Invited Papers* (pp. 463-466). Delft University Press.

Document status and date:
Published: 01/01/1995

Document Version:
Publisher's PDF, also known as Version of Record (includes final page, issue and volume numbers)

Please check the document version of this publication:

• A submitted manuscript is the version of the article upon submission and before peer-review. There can be important differences between the submitted version and the official published version of record. People interested in the research are advised to contact the author for the final version of the publication, or visit the DOI to the publisher's website.
• The final author version and the galley proof are versions of the publication after peer review.
• The final published version features the final layout of the paper including the volume, issue and page numbers.

Link to publication

General rights
Copyright and moral rights for the publications made accessible in the public portal are retained by the authors and/or other copyright owners and it is a condition of accessing publications that users recognise and abide by the legal requirements associated with these rights.

• Users may download and print one copy of any publication from the public portal for the purpose of private study or research.
• You may not further distribute the material or use it for any profit-making activity or commercial gain
• You may freely distribute the URL identifying the publication in the public portal.

If the publication is distributed under the terms of Article 25fa of the Dutch Copyright Act, indicated by the "Taverne" license above, please follow below link for the End User Agreement:

www.tue.nl/taverne

Take down policy
If you believe that this document breaches copyright please contact us at:

openaccess@tue.nl

providing details and we will investigate your claim.

Download date: 04. Oct. 2023

CAD-TOOL FOR INTEGRATED OPTICS

X.J.M. Leijtens, L.H. Spiekman, C. van Dam, L.C.N. de Vreede, M.K. Smit, J.L. Tauritz
Laboratory for Telecommunication and Remote Sensing Technology,
Delft University of Technology, P.O. Box 5031, 2600 GA Delft, The Netherlands,
Tel. +31-15-787089, Fax. +31-15-784046

Abstract – A CAD-tool for simulation and design of integrated optical circuits, based on a professional microwave design system is reported. An example describing the complete design and simulation of a MZI switch is given.

Introduction

Computer aided design tools for integrated optical circuits are far less developed than their microwave counterparts. In general commercially available tools initiate the design and simulation based on a physical description of the circuit and use BPM based computational techniques to carry out the simulation. Computer aided design tools for microwave integrated circuits use a more abstract

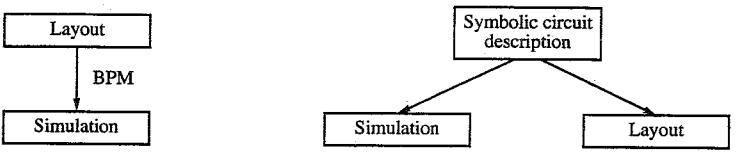

Figure 1: BPM simulation from physical description (left). Simulation and layout generation from a symbolic description (right).

approach initiating the design on a symbolic level. From this level the simulation is performed and the layout is generated (see Fig. 1). The advantage of this approach is that the circuit can be better structured and that one can choose both BPM and other simulation methods for different components or subcircuits. Realizing that integrated optical circuits are conceptually quite similar to microwave integrated circuits, we have chosen to adapt a professional microwave design system, Hewlett Packard's MDS, for the CAD of optical chips [1].

General features

HP's MDS provides a graphical interface for building circuits with standard or user-defined components. MDS performs (multi-) parameter sweeps and automatic (multi-) parameter optimizations. The simulation results can be processed and presented on screen, or exported to other applications. Mask layout can be (automatically) generated, manipulated and viewed on screen.
Subcircuits can be grouped into new circuit components facilitating hierarchical designs. User supplied models written in `C`, `C++` or `FORTRAN` can be used to calculate the component's scattering matrix S. These models are linked with the standard MDS component library and can be used in an identical fashion. We have implemented a series of user-compiled models to realize the optical simulator.

Description of optical components

The coupling between optical components may take place via guided modes and radiation fields. If coupling through radiation fields can be neglected, optical components may be seen as individual units connected to each other at well defined ports. In this concept, the response of an N-port component can be described by its $N \times N$ S-matrix. For each guided mode one port is used.
An ideal monomode waveguide is a 2-port component described by a 2×2 scattering matrix with $S_{11} = S_{22} = 0$. The junction between two monomode waveguides is described by a 2×2 scattering

	straight waveguide	curved waveguide	waveguide junction
graphical representation	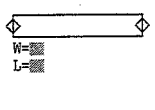	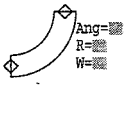	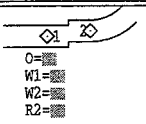
S-matrix	$\begin{pmatrix} 0 & e^{-j\beta\ell} \\ e^{-j\beta\ell} & 0 \end{pmatrix}$	$\begin{pmatrix} 0 & e^{-j\beta_\phi\phi} \\ e^{-j\beta_\phi\phi} & 0 \end{pmatrix}$	$\begin{pmatrix} 0 & \int U_1 U_2^* \\ \int U_1 U_2^* & 0 \end{pmatrix}$

Table 1: Graphical representation and S-matrix description of monomode waveguide components.

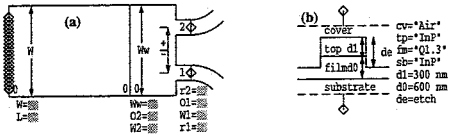

Figure 2: **(a)** Multimode waveguide and junction connecting to two curved waveguides. **(b)** Component used for specifying the waveguide structure.

matrix. The matrix elements are given by the overlap integral of the modal fields, U_1 and U_2, in each of the waveguides: $S_{12} = S_{21} = \int U_1 U_2^*$. As reflections in optical chips are usually small, we assumed that $S_{11} = S_{22} = 0$ for the junctions as well, although inclusion of reflections is straightforward. The basic elements are summarized in Table 1. The parameter list attached to each component specifies the geometry. Figure 2(a) shows an example of a multimode waveguide attached to a junction connecting it to two curved monomode waveguides. The scattering matrices for the multimode waveguides and junctions can be determined based on calculations of the modal propagation constants β_ν and the corresponding modal field distributions U_ν.

As a first step we implemented the Effective Index Method [2] in combination with the Transfer Matrix Method [3] for determining the propagation constants and modal fields in straight waveguides. For curved waveguides we use a conformal transformation as proposed by Heiblum and Harris [4]. This method has the advantage of high computational speed and is well suited for parameter sweeps. It can, however, not be used for simulating continuous junctions (e.g. Y-junctions, directional couplers or tapers), where the BPM would be more suited. The University of Twente in the Netherlands has succesfully implemented a 2D BPM [5] for simulating tapers in MDS.

A special component specifies the layer structure of the waveguides. An example representative of the layer structure of a strip-loaded rib waveguide is shown in Figure 2(b). For each layer the user specifies the thickness and the material used. Each of these parameters can be entered directly, as with for example the film thickness (`d0=600 nm`), or through a variable (`de=etch`).

To enter the material parameters the user can specify the (complex) refractive indices or, in the case of InP/InGaAsP, specify the bandgap wavelength and doping level. The refractive indices of InP/InGaAsP at a given wavelength are calculated using the model of Fiedler and Schlachetzki [6] and take into account the material dispersion.

Design of a Mach-Zehnder interferometer switch

The design of a Mach-Zehnder interferometer (MZI) switch is useful in illustrating the potential of the present approach. The circuit is represented symbolically in Figure 3 and consists of about 50 separate components: straight and curved monomode and multimode waveguides and junctions.

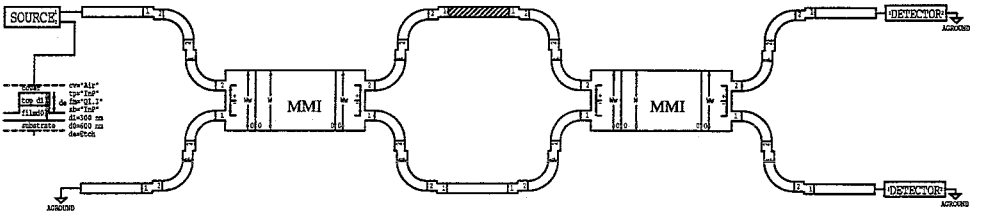

Figure 3: Symbolic representation of the Mach-Zehnder interferometer.

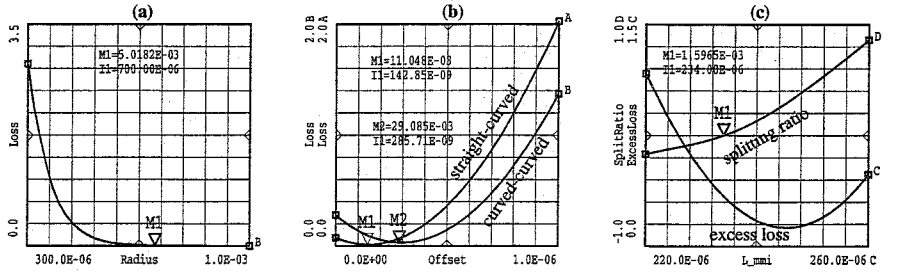

Figure 4: **(a)** Radiation loss (in dB/90°) in curved waveguide as a function of the bending radius. **(b)** Junction loss as a function of the curved-straight and curved-curved waveguide offsets. **(c)** Splitting ratio and excess loss versus the length of the MMI section.

The incoming light is equally distributed into the two arms of the interferometer by the first 2 × 2 multimode interference (MMI) coupler. The second MMI coupler recombines the light into a single output waveguide. If both arms of the MZI are identical, the switch is in the cross state. Introducing a phase shift of π in one of the arms causes a switch to the bar state.

The radius of curvature of the waveguide bends and the optimum offsets between the straight and curved waveguides [7] are first determined. Next the multimode interference (MMI) couplers are designed and finally we simulate the overall switch behavior and generate the mask.

Based on experience a waveguide width of 2 μm is chosen. In order to determine the optimum bending radius, we use a circuit consisting of a curved waveguide and plot the loss as a function of the radius. Figure 4(a) shows the result as it appears on the MDS screen. We choose a conservative value for the radius, 700 μm. We now optimize the offset between a straight and a curved waveguide and between two curved waveguides, and find 0.14 μm and 0.29 μm, respectively (see Fig. 4(b)).

In order to guide a sufficient number of modes we choose the width of the MMI section to be 6.5 μm. The access waveguides are positioned at such that the gap between them is 2.5 μm. We varied the length of the MMI around an estimated value of 240 μm and plotted in Figure 4(c) the excess loss ($-10\log(P_1+P_2)$) and the splitting ratio ($10\log(P_1/P_2)$), where P_1 and P_2 are the normalized optical power at either output. Since we are mostly concerned with a symmetrical operation, we choose L_{MMI} = 234 μm, where $P_1 = P_2$.

All important design parameters having been determined we can now simulate the behavior of the full design. The simulation results[1] as shown in Figure 5, take into account the losses at junctions and radiation losses in curves. Figure 5(a) shows P_1 and P_2 as a function of Δw, the deviation from the design width for all waveguide structures. It is therefore a simulation of the sensitivity for the width

[1]The simulations were done on a (low end) Hewlett Packard HP9000/710 workstation and all simulations shown take less than one minute to perform.

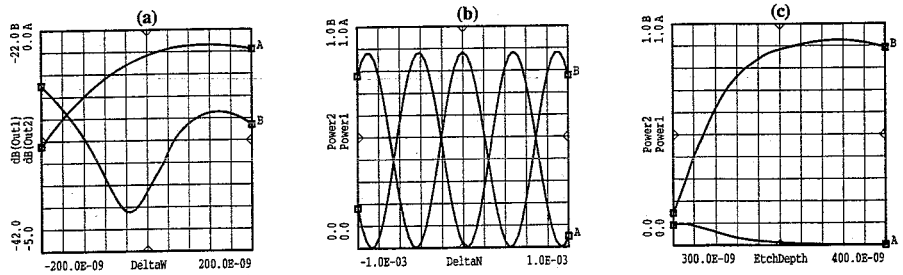

Figure 5: **(a)** Output power (in dB) for the MZI outputs as a function of the structure widths. **(b)** Normalized power at the MZI output ports versus a variation in refractive index in one of the MZI arms. **(c)** Normalized power at the MZI output ports versus the etch depth.

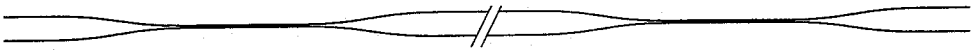

Figure 6: Automatically generated mask.

variations due to lithographic or processing tolerances.
For one of the two waveguides arms in the MZI, shown hatched, the refractive index for the film layer may be varied slightly (for instance by applying an external electric field). Figure 5(b) shows the simulated behavior of the switch as a function of this difference in refractive index.
A critical parameter is the waveguide etch depth which was nominally set to 350 nm. Figure 5(c) shows the normalized power at the output ports as a function of the etch depth, from which the tolerance is directly read.
Mask generation modules have been appended to the optical component models. Figure 6 shows the mask layout directly generated from the symbolically defined circuit.

Conclusion

A powerful CAD-tool for simulation and design of integrated optical circuits based on Hewlett Packard's microwave design system has been developed. It provides a fast and flexible system in which the circuit is described on a symbolic level. The optical behavior of the circuit can be accurately simulated and photolithographic masks can be automatically generated. Work is continuing on the implementation of additional components as well as numerical methods such as 2D BPM and 3D mode solvers.

References

[1] C. van Dam et al. In *Procs. 10th Eur. Conf. on Circuit Theory and Design*, volume III, pages 1316–1323. Polytechnic press, New York, Sept 2–6 1991.
[2] R.M. Knox and P.P. Toulios. In *Proc. Symp. on Submillimeter Waves*, volume XX, pages 497–516. Polytechnic press, New York, March 31–April 2 1970.
[3] K. Thyragarajan et al. *Optics letters*, 12(4):296–298, 1987.
[4] M. Heiblum and J.H. Harris. *IEEE J. Quantum Electron.*, QE-11(2):74–83, Feb 1975. with correction QE-12 p.313.
[5] H.J.W.M. Hoekstra et al. *J. Lightwave Technol.*, 10:1352–1355, 1992.
[6] F. Fiedler and A. Schlachetzki. *Solid State Electron.*, 30(1):73–83, 1987.
[7] E. C. M. Pennings. PhD thesis, Delft University of Technology, Delft, The Netherlands, 1990.